*International Journal of Advanced Smart Convergence Vol.10 No.2 108-122 (2021)*
*http://dx.doi.org/10.7236/IJASC.2021.10.2.108*

**IJASC 21-2-15**

# Precision comparison of 3D photogrammetry scans according to the number and resolution of images

JaeWook Park[1], YunJung Kim[2], Lyoung Hui Kim[3], SoonChul Kwon[4] and SeungHyun Lee[5†]

*[1]Doctoral candidate, Department of Plasma Bio Display, Kwangwoon University, Seoul 01897, Korea*
*[2]Assistant Professor, School of SW Advanced Convergence Technology, Inha University, Incheon 22212, Korea*
*[3]Assistant Professor, Department of Visual Design, Seoul Institute of the Arts, Gyeonggi-do 15263, Korea*
*[4]Associate professor, Graduate School of Smart Convergence, Kwangwoon University, Seoul 01897, Korea*
*[5†]professor, Ingenium College, Kwangwoon University, Seoul 01897, Korea*
*e-mail : {[1]jaewookpark,[4]ksc0226,[5†]shlee}@kw.ac.kr,[2]yunjkim@inha.ac.kr,[3]rhkim@seoularts.ac.kr*

***Abstract***

*With the development of 3D graphics software and the speed of computer hardware, it is an era that can be realistically expressed not only in movie visual effects but also in console games. In the production of such realistic 3D models, 3D scans are increasingly used because they can obtain hyper-realistic results with relatively little effort. Among the various 3D scanning methods, photogrammetry can be used only with a camera. Therefore, no additional hardware is required, so its demand is rapidly increasing. Most 3D artists shoot as many images as possible with a video camera, etc., and then calculate using all of those images. Therefore, the photogrammetry method is recognized as a task that requires a lot of memory and long hardware operation. However, research on how to obtain precise results with 3D photogrammetry scans is insufficient, and a large number of photos is being utilized, which leads to increased production time and data capacity and decreased productivity. In this study, point cloud data generated according to changes in the number and resolution of photographic images were produced, and an experiment was conducted to compare them with original data. Then, the precision was measured using the average distance value and standard deviation of each vertex of the point cloud. By comparing and analyzing the difference in the precision of the 3D photogrammetry scans according to the number and resolution of images, this paper presents a direction for obtaining the most precise and effective results to 3D artists.*

***Key words:*** *3D Scan, Image Resolution, Photogrammetry, Point Cloud, Retopology, 3D Modeling*

## 1. INTRODUCTION

With the advancement of three dimensional (3D) graphics software and the improvement of computer hardware speed in this era, we can realistically express not only movie visual effects but also console games. In the production of such realistic 3D models, 3D scans are increasingly used because they can obtain ultra-realistic results with relatively little effort. Among the various 3D scanning methods, photogrammetry can be used only with a camera, hence without the need for additional hardware, so its demand is rapidly increasing. However,

Manuscript Received: May. 3, 2021 / Revised: May. 5, 2021 / Accepted: May. 10, 2021
Corresponding Author: shlee@kw.ac.kr
Tel: +82-2-940-5290, Fax: +82-2-940-5443
Graduate School of Information Contents, Kwangwoon University, Korea

research on how photogrammetry can obtain more precise results is lacking, and there is no research on how precision relates to the number of images.

G. Tucci *et al.* scanned shapes of sculptures through a photogrammetry method. In this study[1], it is meaningful to measure the precision of each part of the scanned sculpture, but the cause of the location affecting the precision could not be identified. Luigi Maria Galantucci *et al.* has eliminated optical aberration issues and has been proposed a robust validation method, for photogrammetric scanning systems[2]. However, optical aberration issues did not significantly affect the accuracy of the scan. Rachel Opitz *et al.* studied a comparison of at least three photogrammetric software packages including Eos Systems' PhotoModeler Scanner, AutoDesk's 123D Catch and AgiSoft's PhotoScan[3]. This is to compare the results by software using the same data, but there was no study comparing the precision of the data and the results. Gianluca Percoco *et al.* studied the measurement of small objects with micro-features necessary for 3D microscopy, and obtained experimental results that photogrammetric scanning obtains good results even on small objects[4]. However, there was no analysis of the causes affecting the precision. Hafeez *et al.* investigated the precision of each texture by using different textures on the subject of the photogrammetry, and found that there was a difference in the precision according to the type of each texture[5]. Choi and Jongho *et al.* proposed a method for 3D reconstruction by photogrammetry even in the presence of motion blur and degenerate motions[6]. Lee, Geon-hee *et al*. studied the difference in performance by comparing different 3D file formats[7]. Hwang and Leehwan *et al*. obtained the result in their study that the higher the number of meshes used in cubic meters, the higher the accuracy between real space and spatial mapping[8]. Kwon and Soon Chul *et al.* studied how to obtain depth to convert 2D to 3D, and in particular, studied how to increase the depth resolution through the pixel bundling method[9].

Many producers take as many images as possible with a video camera and then calculate using all the images, so the task requires a lot of memory and long hardware calculations[10][11].

In this study, we compared and analyzed the difference in the precision of 3D photogrammetry scans according to the number and resolution of images. This paper is organized as follows: In Section 2, research on the photogrammetry production method and work stage is reviewed. In Section 3, point cloud data generated according to the number of images and resolution are presented, and an experiment conducted to compare the results with original data is discussed. In Section 4, the experimental results are explained. In Section 5, conclusions are presented.

## 2. THEORETICAL BACKGROUND

### 2.1 Photogrammetry

Photogrammetry is a scanning method generally based on the structure from motion. Figure 1 shows the main variables used in photogrammetry.

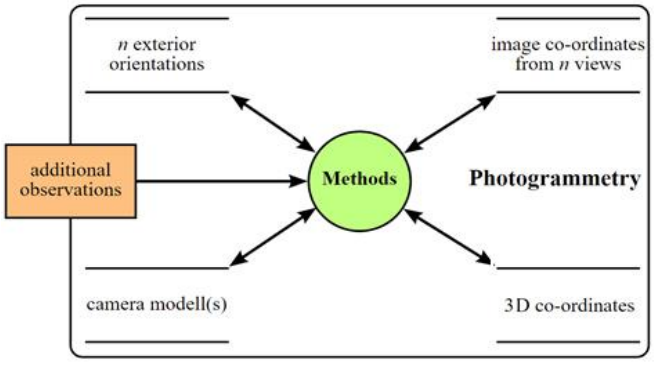


**Figure 1. Key variables in photogrammetry [12].**

3D coordinations define the location of feature points in a 3D space. Image coordinations define the two dimensional (2D) position of a feature point on a film or screen. The camera's exterior orientations define its position and view direction in space. The camera model defines the geometric parameters of the image formation process. This is primarily the focal length of the lens, but it may also include an explanation of lens distortion. Further observation also serves to set the standard for size. Basically, this is the distance value obtained by measuring two points in space. Each of the main variables in Figure 1 can be an input or result of photogrammetry. Figure 2 shows a 3D scan using photogrammetry and its main variables.

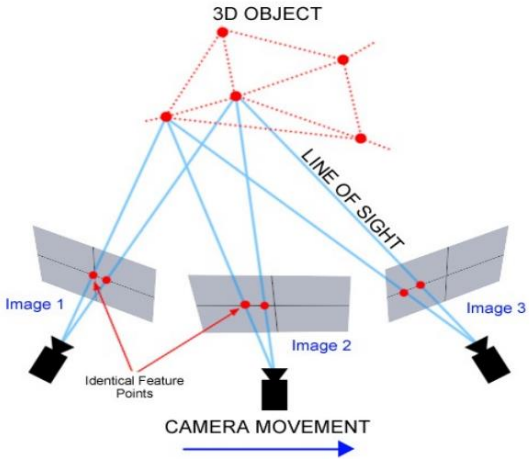


**Figure 2. 3D scanning using photogrammetry [13]**

Based on the image captured by the camera, feature points are extracted using triangulation technology to create a point cloud, and then the mesh is reconstructed. Photogrammetry is operated based on SfM, which can be used to extract 3D coordinates using the motion of the image. SfM has four major process steps. The first step involves camera calibration, wherein the determinant of the camera is calculated through information on the camera's position, rotation, focal length, and sensor size. The second is to extract points from images. Then, the dimensional coordinates are extracted, and finally the mesh is reconstructed. Each procedure is described as follows.

### 2.1.1 Extraction of Image Feature Points

Camera calibration was prepared for the projection matrix in order to calculate the 3D world coordinates of the point of view of two cameras. Equation 1 is expressed for the camera matrix M.

$$M = K[R \quad T] \tag{1}$$

Here, it may be expressed as a rotation matrix R and a position coordinate T of the camera and an intrinsic matrix K containing information, such as focal length and sensor size. Equation 2 represents matrix K[14]:

$$K = \begin{bmatrix} a_x & \gamma & u_0 & 0 \\ 0 & a_y & v_0 & 0 \\ 0 & 0 & 1 & 0 \end{bmatrix} \tag{2}$$

$a_x$ and $a_y$ are represented by $a_x = f \cdot m_x$ and $a_y = f \cdot m_y$, respectively, and denote a focal length. $u_0$ and $v_0$ represent the 2D position in the center of the image. The matrix for converting the 3D coordinates to the camera coordinate system using rotation R and movement T is expressed in Equation 3:

$$\begin{bmatrix} R_{3\times3} & T_{3\times3} \\ O_{3\times3} & 1 \end{bmatrix}_{4\times4} \tag{3}$$

The feature point extraction of an image means extracting a key point so that feature points between each

image can be matched in an image.

For an image feature to be considered good, it should be easily identified even if the size and position of an object change, and the point in the image should be easily found even if the viewpoint and lighting of the camera change. These feature point extraction algorithms include Harris corner detector, Shi–Tomasi method, scale invariant feature transform difference of Gaussian (SIFT-DoG) method, and features from accelerated segment test (FAST) method. The image of the difference value obtained by subtracting the brightness value of the image between adjacent Gaussian blur images after applying Gaussian blur to the original image in each step is called DoG. A bundle of DoGs obtained from an image of one resolution is called an octave. This process consists of several octaves, which reduces the resolution by half. The horizontal axis of the image above represents the increase in the intensity of the Gaussian blur, whereas the vertical axis represents the pyramid configuration with the resolution reduced by half. Figure 3 shows the DoG results with the difference between adjacent Gaussian blur images.

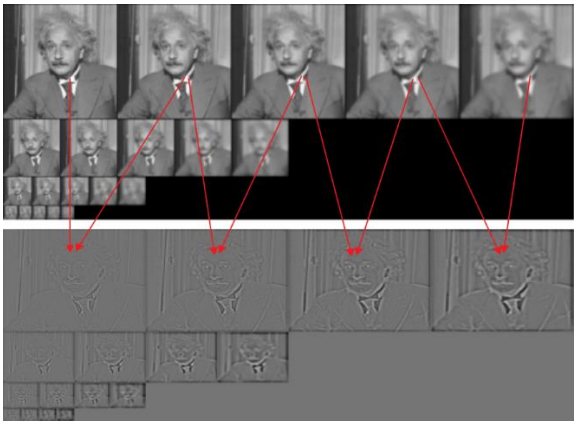

**Figure 3. DoG results showing the difference between adjacent Gaussian blur images.[15]**

At every octave step of the obtained DoG pyramid, the maximum or minimum points were compared to extract the feature points, and then the noise feature points were removed. Then, a direction histogram was obtained for the feature point, and the strongest direction was determined as the direction of the feature point. Accordingly, each feature point has a position, scale, and direction. All information was then extracted based on these values. Figure 4 shows the location, scale, and direction of each feature point for which the extracted feature point and direction are determined.

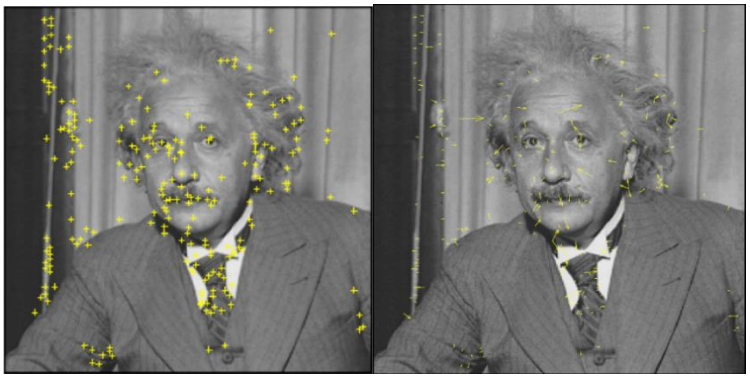

(a) (b)

**Figure 4. Post processing for each feature point in the DoG results: (a) extracted feature point; (b) location, scale, and direction of each feature point whose direction is determined.[15]**

### 2.1.2 Mesh Reconstruction

The feature point extracted from the image was obtained through triangulation using the 2D coordinates of the feature point in each image and the camera correction value. Figure 5 shows the process of extracting 3D coordinates.

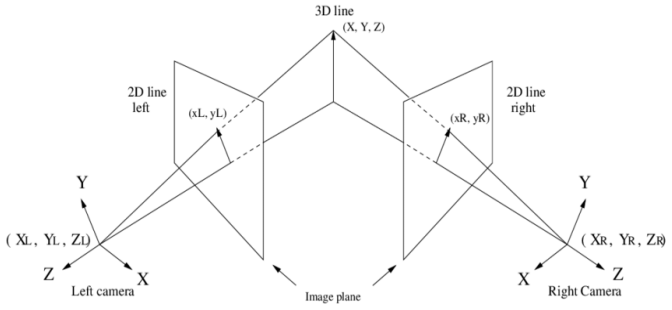


**Figure 5. Process of extracting 3D coordinates**

Each image coordinate includes P 1 (u 1, v 1) and P 2 (u 2, v 2), f is the focal length, and P (x p, y p, z) is the spatial coordinate obtained via triangulation.

Poisson surface reconstruction algorithm was used to obtain a polygonal mesh by connecting feature points converted to 3D coordinates. This algorithm creates a set of points, estimates a normal vector that can distinguish the inside and outside of the face, and then creates a triangular mesh surface. Each vertex of the point cloud may have sparse parts depending on the number of images and the angle of the camera. In this case, the surface was filled with the nearest vertex as a reference.

## 3. EXPERIMENT

Complex forms of natural objects were 3D scanned using photogrammetry. After 3D scanning with different image counts and resolutions, the differences with the original were compared.

If you take a picture of a natural object and perform a 3D scan using photogrammetry, there is no way to accurately compare the difference between the original object and the photogrammetry-scanned data. Later, the results of the 3D photogrammetry scan with the rendered image were compared with the original.

### 3.1 Comparison Method of the 3D Model Reconstruction According to the Number of Images

#### 3.1.1 Creating Images for Scanning

Datasets were prepared by making images for scanning. The width, depth, and height of the original object are 244.972, 95.473, and 137.343 cm, respectively. The number of images for comparison was reduced to the set of 4 images from the set of 512 images to 21/n each, resulting in a total of 12 image datasets.

For each image dataset, the first comparison target group was created by extracting feature points, aligning cameras, and generating point clouds using RealityCapture(Capturing Reality ltd.).

For mesh reconstruction operation, point clouds created by photogrammetry change the size of the mesh for a specific area according to its density. So the free open source tool Instant Meshes is used to fill point clouds at equal intervals even in empty areas. After entering, a 3D mesh was created to construct a second group to be compared.

The generated 3D mesh was created using CloudCompare 2017, an open source tool to compare and evaluate method. The average distance of the interval was obtained by considering the original 3D mesh, which is the basis of comparison, as the ground truth data, and comparing the position coordinates of the vertices of the objects belonging to the first and second groups to be compared with the face positions of the original 3D mesh. Then, the standard deviation were calculated.

First, the results obtained by comparing the coordinates of each point in the point cloud, which is the first comparison target group, with the original 3D mesh are shown in Figure 6.

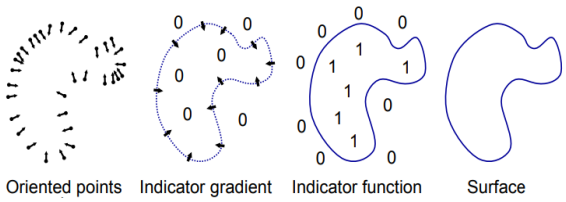


**Figure 6. Intuitive illustration of Poisson reconstruction in 2D [16]**

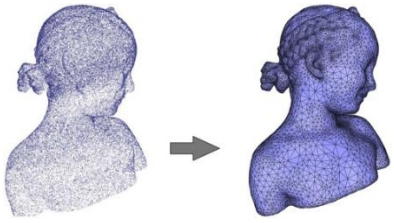

**Figure 7. Poisson reconstruction [17]**

Comparing point cloud, from the results of the 3D model using the 512 images in the upper left corner, a 3D model was obtained using half an image for each step. Then, the location of each vertex (point cloud) of the 3D model and the distance between the original data were calculated and each vertex. The average distance distribution and standard deviation from the nearest value were calculated and are summarized in Table 1.

**Table 1. Average distance distribution and standard deviation from the nearest value**

| Number of images | Average distance (cm) | Standard deviation (cm) |
|---|---|---|
| 512 | 0.00253121 | 0.0702087 |
| 256 | 0.00373586 | 0.0852505 |
| 128 | 0.00332984 | 0.0908906 |
| 64 | 0.00321568 | 0.0809308 |
| 32 | 0.0030042 | 0.0772707 |
| 16 | 0.0030042 | 0.0772707 |
| 8 | 0.00290117 | 0.0776054 |
| 4 | 0.00450589 | 0.107686 |

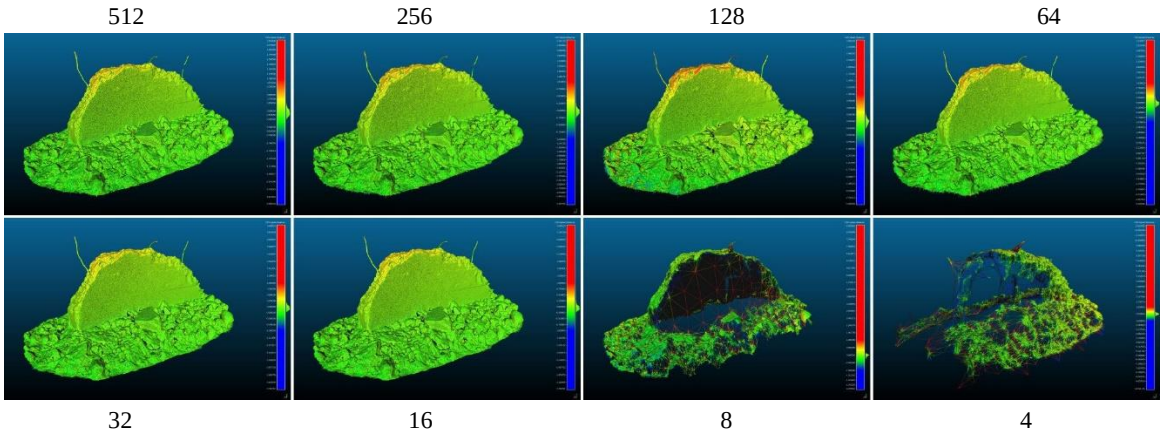


**Figure 8. Source images for photogrammetry scans**

As shown in Figure 8, the number of source images for photogrammetry scans from 512 to 16 visually did not significantly change, but when set of 8 images and set of 4 images were used, a large change was confirmed visually. Moreover, there was an empty space because the number of images was insufficient and the vertex in the direction was not created.

In Table 1, when the largest number of images (512) was used, the average distance was 0.002531 cm, and the average distance of the vertices using the smallest number of images (4) was 0.0045058 cm. This shows the average distance increase of 1.78 times. The standard deviation was 0.0702 cm for the set of 512 images and 0.1076 cm for the set of 4 images, signifying an increase of 1.53 times. In Figure 8, when 8 and 4 images were used, there was a big change in the shapes visually, but the average distance and standard deviation of each vertex showed a small difference in a degree not related to the visual change.

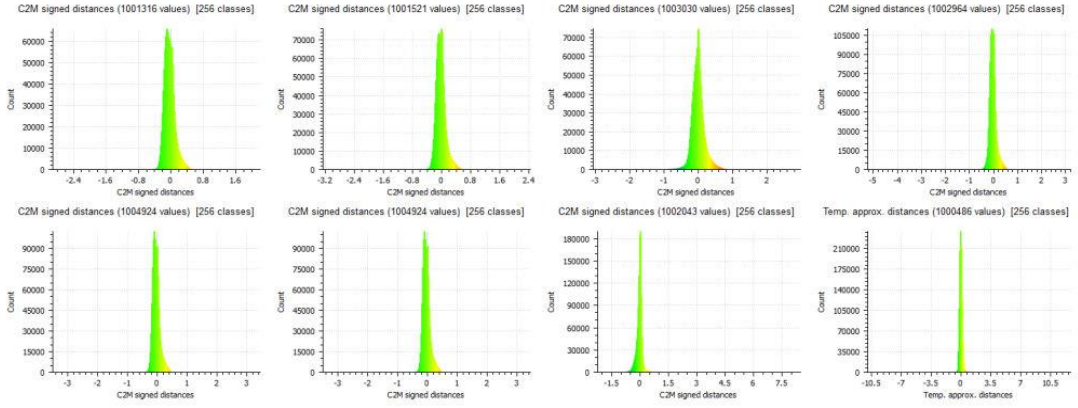


**Figure 9. Histogram of the measured distance values according to the number of photos**

Figure 9 is a histogram of the measured distance values, where the X axis represents the distance from the reference point, and the Y axis represents the number of measured vertices. Again, as shown in Table 1, the average distance of each vertex has no significant correlation with the number of images.

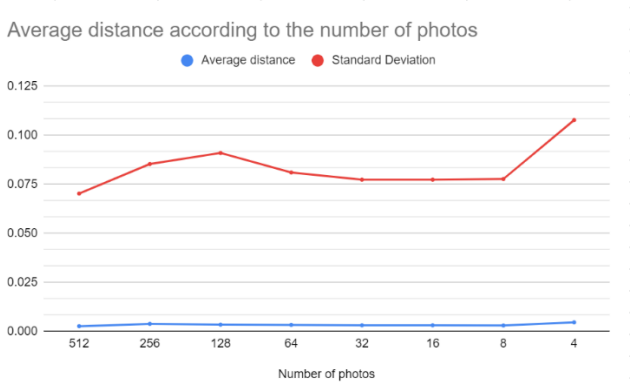


**Figure 10. Graph of the average distance according to the number of photos**

In Figure 10, a graph using the values in Table 1 is presented. The horizontal axis is the number of images for generating the point cloud, and the vertical axis is the distance. The dark blue graph at the bottom is the average distance value of the point cloud, and the red graph at the top is the standard deviation value.

On the horizontal axis, the number of images decreased by half, but the average distance and standard deviation of the point cloud had insignificant effect on the number of images. In Figure 8, the point cloud created using the set of 4 images on the right shows a big difference visually, considering the many empty spaces because there are no images compared to the original mesh on the left. However, the empty space itself did not affect the mean distance value or standard deviation value.

That is, when the number of images is small, a point cloud may not be created in a specific area in the square of the images used, and thus an empty space may be created in the point cloud. The average distance and standard deviation of the point cloud were constant regardless of the number of images

### 3.2 Reconstructed Point Cloud Comparison

The results obtained by comparing the polygon mesh obtained through the retopology of the second comparison target group and point cloud data at equal intervals, with the original 3D mesh are presented as follows. Unlike the first comparison target group, the second comparison target group was compared with the original data, whereas the empty point cloud areas were filled in equally spaced.

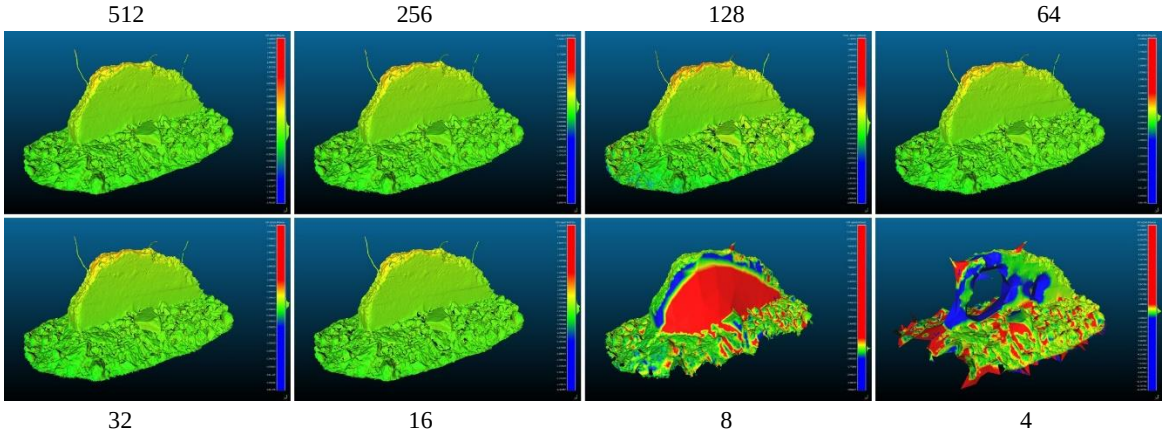


**Figure 11. Point cloud distance value displayed in color.**

In Figure 11, in the case of data created using set of 8 images and set of 4 images, the difference in the shape from the original is visually revealed as the point cloud is filled in the existing empty area.

**Table 2. the average distance distribution and standard deviation of each vertex of the second comparison group**

| Set of images | Average distance | Standard deviation |
|---|---|---|
| 512 | 0.00243005 | 0.0685988 |
| 256 | 0.00315457 | 0.0784234 |
| 128 | 0.00368759 | 0.08466545 |
| 64 | 0.00422061 | 0.0909075 |
| 32 | 0.00239229 | 0.0682005 |
| 16 | 0.00271704 | 0.0729771 |
| 8 | 0.453073 | 1.55607 |
| 4 | 0.658373 | 1.74668 |

In Table 2, where the average distance distribution of each vertex of the second comparison group and the standard deviation from the nearest value were calculated, the average distance and standard deviation hardly changed until the number of photos was 16. The results confirmed that the mean distance and standard deviation sharply increased, indicating a significant difference.

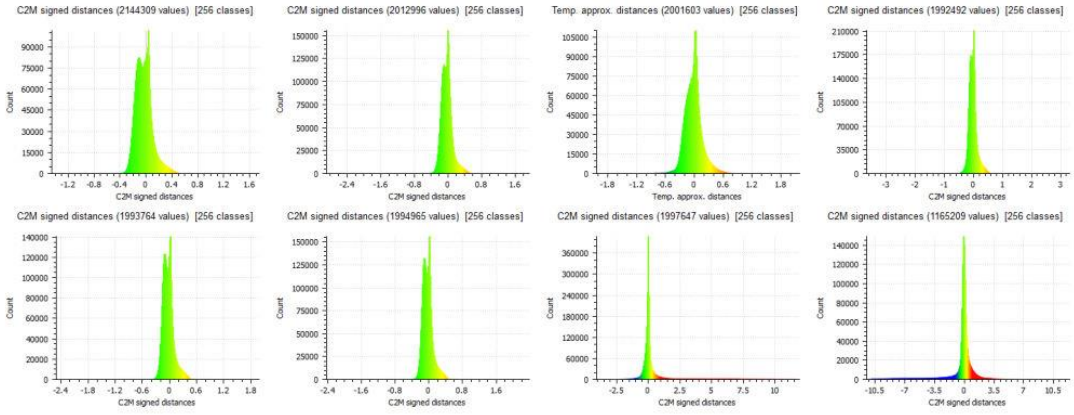


**Figure 12. Histogram of the measured distance values of the reconstructed point cloud comparison**

Figure 12 shows the change more visually than in Table 2. When the number of pictures is set of 8 images and set of 4 images, the horizontal axis of the histogram, that is, a red area with a difference of 1 cm or more outward and a blue area with a difference of 1 cm or more inward can be identified. In Table 2, when the number of photos is 8, the average distance value from the original is 0.453 cm and the standard deviation is 1.556 cm. In the actual point cloud, some vertices with a distance value of 5 cm or more, and vertices over 10 cm were also identified.

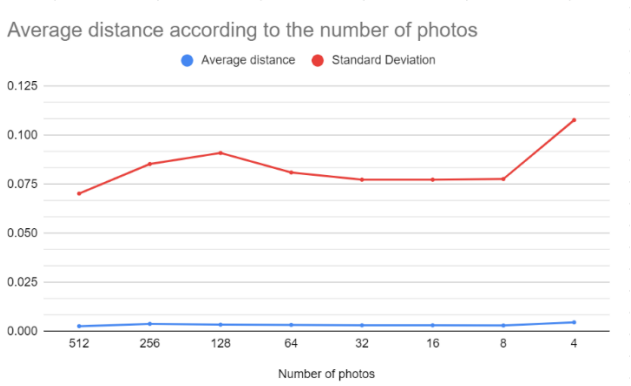


**Figure 13. Average distance according to the number of images**

In Figure 13, which created a graph using the values in Table 2, the slope of the graph was kept constant from 512 to 16 regardless of the number of images, and then an empty space in the point cloud was created, which was filled through the retopology process. The graph goes up from the set of 8 images.

### 3.3 3D Model Reconstruction Comparison Method According to the Image Resolution

Datasets were prepared by making images for scanning. The width, depth, and height of the original object are 4,145, 1,655, and 4,129 mm, respectively. The image resolution for comparison was reduced from 4096 x 4096 pixels to 64 x 64 pixels each by 21/n, resulting in a total of seven levels of image datasets. With using Photogrammetry, point cloud was created. Each image dataset uses RealityCapture from Capturing Reality to extract feature points, align cameras, and create point clouds to create the first comparison target group. The generated 3D mesh was created using CloudCompare 2017, an open source tool to compare and evaluate method. The original 3D mesh, which is the basis for comparison, was regarded as the ground truth data. The average distance and standard deviation of the obtained intervals were calculated by comparing the position coordinates of the vertices of the object belonging to the comparison target group with the plane position of the original 3D mesh.

First, the results obtained by comparing the coordinates of each point in the point cloud, which is the first comparison target group, with the original 3D mesh are shown in Figure 14. From the results of the 3D model using the image with 4096 x 4096 resolution, the 3D model was obtained using half resolution images in each step. Then, the position of each point cloud of the 3D model and the distance between the original data and the average of each vertex were calculated. The standard deviation from the nearest value to the distance distribution was calculated and is summarized in Table 3.

**Table 3. Standard deviation from the nearest value to the distance distribution**

| Image resolution | Number of polygons | Avg dist. | Sigma |
|---|---|---|---|
| 4K | 4425770 | 0.00815731 | 0.517925 |
| 2K | 1999990 | 0.0429001 | 1.18711 |
| 1K | 256840 | 0.559637 | 4.25377 |
| 512 | 60910 | 4.64749 | 11.5107 |
| 256 | 15184 | 17.3438 | 20.5272 |
| 128 | 3554 | 46.2178 | 40.6311 |
| 64 | 774 | 119.421 | 100.135 |

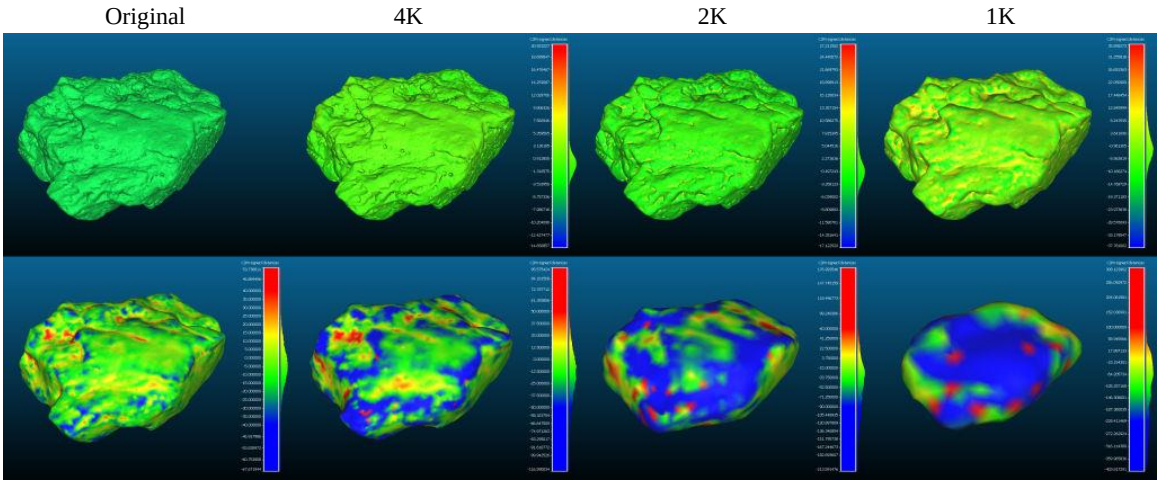


**Figure 14. Shape and change of the surface color according to each step.**

Figure 14 shows the simplification of the shape and the change of the surface color according to each step, from the resolution of the source image for photogrammetry scanning from 4096 x 4096 to 64 x 64. Green indicates the part that matches the original object in color, and blue indicates that the object's polygon is located inside the original surface, and red indicates that the object's polygon is located outside the original surface.

When the image resolution is 1K, a little yellow appears on the surface of the object, and when the image is 512 pixels, the details of the small bumps are compressed and expressed in red or blue. At 128 pixels or less, most of the object is covered with a high-saturation blue, and it can be seen that the shape deformation has occurred significantly.

In Table 3, the average distance when using the highest resolution (4096 x 4096) is 0.0081573 mm, and the average distance of the vertices using the lowest resolution (64 x 64) is 119.42 mm, which is approximately 1.78 times longer. The standard deviation was 0.517925 mm at the highest resolution and increased by approximately 659 times to 100.135 mm at the lowest resolution.

In addition, the image resolution was proportional to the number of extracted 3D polygons. When the highest resolution (4096 x 4096) was used, the number of polygons was 4,225,770, and the number of polygons at the vertex using the lowest resolution (64 x 64) was 774, which is 4096 pixels. At a resolution of 5,459 times, the number of polygons was confirmed. Because the number of pixels with a resolution of 4096 x 4096 is 16,777,216, the ratio of the number of generated polygons to the number of pixels can be calculated as approximately 26.37%. The ratio of the number of polygons extracted for each resolution is as follows.

**Table 4. Ratio of the number of polygons extracted for each resolution**

| Image resolution | Number of pixels | Number of polygons | Pixel ratio to number of polygons |
|---|---|---|---|
| 4K | 16777216 | 4425770 | 0.263796 |
| 2K | 4194304 | 1999990 | 0.476835 |
| 1K | 1048576 | 256840 | 0.244942 |
| 512 | 262144 | 60910 | 0.232353 |
| 256 | 65536 | 15184 | 0.231689 |
| 128 | 16384 | 3554 | 0.216919 |
| 64 | 4096 | 774 | 0.188965 |

The average value of the ratio of pixels to the number of polygons is 0.2651, and the standard deviation is 0.096217. 26.5% of the number of input pixels was generated with a deviation of approximately 1%.

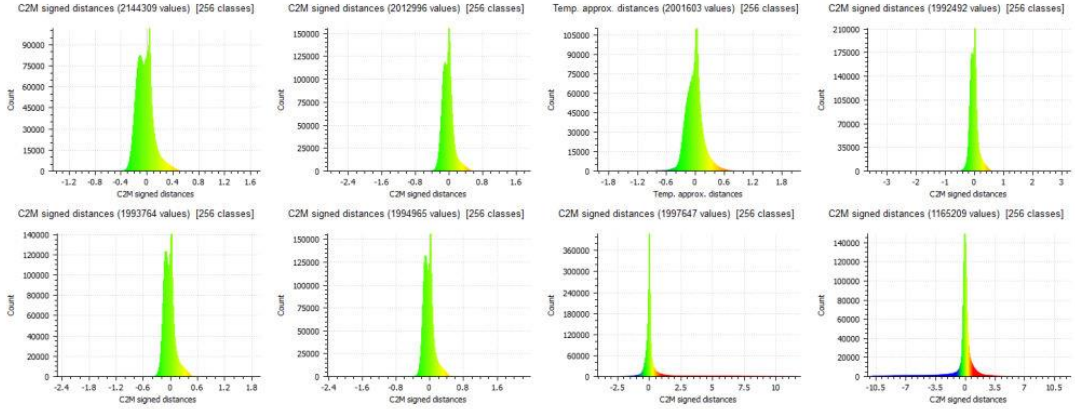


**Figure 15. Histogram of the measured distance values**

Figure 15 is a histogram of the measured distance values, where the X axis represents the distance from the reference point and the Y axis represents the number of measured vertices. The higher the image resolution, the denser the distance value, the lower the average distance value and the maximum distance value, and the smoother the graphs due to the number of polygons. Moreover, the lower the resolution, the rougher the graphs appear due to the lower number of polygons, and the higher the average and maximum distance values.

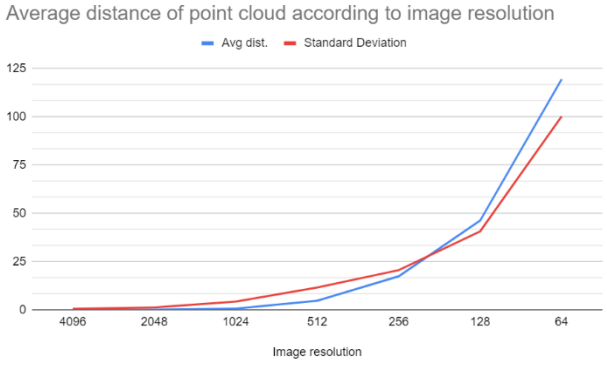


**Figure 16. Average distance of point cloud according to image resolution**

In Figure 16, a graph using the values in Table 3 is presented. The horizontal axis is the number of images for generating the point cloud, and the vertical axis is the distance. The dark blue graph at the bottom is the average distance value of the point cloud, and red graph at the top is the standard deviation value.

On the horizontal axis, the number of images decreased by half, but the average distance and the standard deviation of the point cloud had insignificant effect on the number of images. In Figure 17 the point cloud created using four images on the right shows a big difference visually because there are many empty spaces because there are no images compared to the original mesh on the left. However, the empty space itself did not affect the mean distance value or standard deviation value.

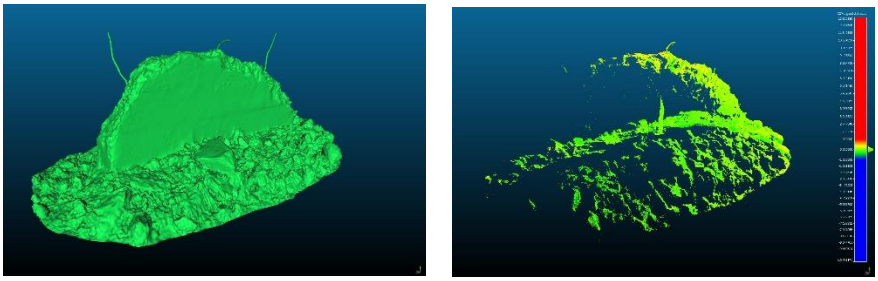

**Figure 17. Point cloud obtained by 3D scanning with the original 3D mesh and four images.**

That is, when the number of images is small, a point cloud may not be created in a specific area in the square of the images to be used, so an empty space may occur in the point cloud. However, once created, the average distance value and standard deviation of the point cloud are constant regardless.

## 4. EXPERIMENTAL RESULTS

In this experiment, a point cloud scanned by photogrammetry, which is one of the 3D scanning methods, and a point cloud retopologized thereto were created. In the photogrammetry scans, starting from the point cloud generation using 512 images, the number of images was reduced in half by each step, and an experimental comparison group of eight steps was created up to four sheets.

Two comparison groups were used in the experiment. The first comparison group was the original point cloud created by photogrammetry. In the point cloud using eight and four images, the number of vertices was not generated due to the insufficient number of images. It was confirmed that there was a sparse empty space.

The second comparison group prepared a newly created point cloud via retopology processing the point cloud of the first comparison group and filling the empty space of the point cloud. Then, using CloudCompare, the distance value of how far each vertex of the point cloud was compared to the original calculated value, the average distance value and the standard deviation between each comparison group were calculated, and then each value was graphed.

In the first comparison group, the average distance from 512 sheets with the largest number of images to four sheets with the smallest number of images was 0.0025 cm to 0.0045 cm, showing a small difference that is almost meaningless compared to the total width of the comparison object, i.e., 244.972 cm. The standard deviation was also 0.07 cm for 512 images and 0.107 cm for 4 images, indicating a difference value that could be seen regardless of the number of images. The empty space of the point cloud occurs when the number of images is insufficient, so triangulation from the image is not possible. This finding could be confirmed through the comparison group. There was no significant difference in the second comparison group up to the number of images in which no empty space was created in the point cloud. However, there was a visually empty space in the point cloud form was found in the set of 8 images and the set of 4 images that were filled with retopology. In the set of 8 images and the set of 4 images, the average distance was 0.453cm and 0.658cm, showing a big difference from the result of 512 photos, which was 0.002cm. The standard deviation was 1.556cm and 1.747cm at the set of 8 images and the set of 4 images, showing a big difference from 0.068cm, which is the result of 512 photos.

In the experiment in the second comparison group, the difference between the mean distance value and standard deviation of the results of using 16 images and 512 sheets showed the minimum results except for the data of chapters of 8 images set and 4 images set. The result values were different from those of retopology, which did not come up with a significant value.

In other words, the results show that the precision of photogrammetry is not proportional to the number of images and the precision of results as long as only the number of images is secured, such that no empty space in

the point cloud is created.

## 5. CONCLUSIONS

In 3D scan data, photogrammetry can obtain scan data with only a camera, hence without the need for expensive scanning equipment. Accordingly, the demand for computer graphic assets for movies and games has significantly increased in recent years. However, because there is no guide for obtaining precise results with photogrammetry, production is made with a large number of photos, which leads to an increase in production time and a decrease in productivity due to an increase in data capacity. In this study, to determine the most effective image number in photogrammetry scanning by comparing point cloud data obtained using different image numbers, precision was measured using the average distance value and standard deviation of each vertex of the point cloud. In photogrammetry, the precision of each vertex of the point cloud once created was able to confirm consistent precision regardless of the number of images. In addition, when the point cloud for a specific surface cannot be created due to the insufficient number of images, the precision when the point cloud is not created for a specific surface is significantly lowered when it is made into a surface through retopology. Our results confirmed that 16 images, which is the minimum number of images that can be generated on each side, is the number of images with the best productivity versus precision.

Photogrammetry allows individuals to easily obtain 3D scan data. Therefore, it can be expected that the field of application will be greatly expanded in the future. Thus, the results of this study can be used efficiently by people who perform 3D scans using photogrammetry.

## REFERENCES

[1] G. Tucci, G. Guidi, D. Ostuni, F. Costantino, M. Pieraccini, and J.-A. Beraldin, "Photogrammetry and 3D Scanning: Assessment of Metric Accuracy for the Digital Model of Danatello's Maddalena," *Proceedings of the 2001 Workshop of Italy-Canada on 3D Digital Imaging and Modeling Application of: Heritage, Industry, Medicine, and Land,Padova*, April 2001.

[2] Galantucci, Luigi & Lavecchia, Fulvio & Percoco, Gianluca & Raspatelli, Sergio, "New method to calibrate and validate a high-resolution 3D scanner based on photogrammetry," *Precision Engineering*, Volume 38, Issue 2, pp. 279-291, April 2014.
DOI:https://doi.org/10.1016/j.precisioneng.2013.10.002

[3] Rachel Opitz, Katie Simon, Adam Barnes, Kevin Fisher, Lauren Lippiello, "Close-range photogrammetry vs. 3D scanning: Comparing data capture," *processing and model generation in the field and the lab. The Computer Applications and Quantitative Methods in Archaeology (CAA) 2012 Conference*, 2012.

[4] Percoco, G., Guerra, M.G., Sanchez Salmeron, A.J, "Experimental investigation on camera calibration for 3D photogrammetric scanning of micro-features for micrometric resolution," *Int J Adv Manuf Technol 91*, pp. 2935–2947, August 2017.
DOI:https://doi.org/10.1007/s00170-016-9949-6

[5] J. Hafeez, S. Lee, S. Kwon, and A. Hamacher, "Image Based 3D Reconstruction of Texture-less Objects for VR Contents," International journal of advanced smart convergence, vol. 6, no. 1, pp. 9–17, Mar. 2017. DOI:10.7236/IJASC.2017.6.1.9.

[6] J. Choi, S. Kwon, K. Son, and J. Yoo, "Fast key-frame extraction for 3D reconstruction from a handheld video," International journal of advanced smart convergence, vol. 5, no. 4, pp. 1–9, Dec. 2016.
DOI: https://doi.org/10.7236/IJASC.2016.5.4.1

[7] G. Lee, P. Choi, J. Nam, H. Han, S. Lee, and S. Kwon, "A Study on the Performance Comparison of 3D File Formats on the Web," International journal of advanced smart convergence, vol. 8, no. 1, pp. 65–74, Mar. 2019.
DOI: http://dx.doi.org/10.7236/IJASC.2019.8.1.65

[8] L. Hwang, J. Lee, J. Hafeez, J. Kang, S. Lee, and S. Kwon, "A Study on Optimized Mapping Environment for Real-time Spatial Mapping of HoloLens," International Journal of Internet, Broadcasting and Communication, vol. 9, no. 3, pp. 1–8, Aug. 2017.
DOI:http://dx.doi.org/10.7236/IJIBC.2017.9.3.1

[9] S. C. Kwon, H. B. Chae, S. J. Lee, K. C. Son, and S. H. Lee, "A Study on Depth Information Acquisition Improved by Gradual Pixel Bundling Method at TOF Image Sensor," International Journal of Internet, Broadcasting and Communication, vol. 7, no. 1, pp. 15–19, Feb. 2015.
DOI:http://dx.doi.org/10.7236/IJIBC.2015.7.1.15

[10] Wiora, "Optical 3D Metrology," Universitätsbibliothek Heidelberg, pp. 36, 2006.
DOI: https://doi.org/10.11588/heidok.00001808

[11] Forest Collado J, "New Methods for Triangulation Based Shape Acquisition using Laser Scanners," Thesis, Universitat de Girona, 2004.

[12] L.H Kim, "A Study of a Photogrammetry Scanning Quality Based on a High Dynamic Range Image," Thesis, Kwangwoon University, pp. 1–95, 2019.

[13] H. Kamel, Youssef Chahir, Mohamed Khireddine Kholladi, "SIFT Detectors for Matching Aerial Images in Reduced Space," IEEE International Conference on Computer Integrated Manufacturing - CIP'2007, 2007, Sétif, Algeria. pp. 10

[14] Richard Hartley and Andrew Zisserman, "Multiple View Geometry in Computer Vision," Cambridge University Press. pp. 155–157, 2003.

[15] Matthew Berger, Andrea Tagliasacchi, Lee Seversky, Pierre Alliez, Gael Guennebaud, "A Survey of Surface Reconstruction from Point Clouds," Computer Graphics Forum, Wiley, pp. 27, 2016
DOI: https://onlinelibrary.wiley.com/doi/10.1111/cgf.12802

[16] Eberhard L.A, Sirguey P, Miller A, Marty M, Schindler K, Stoffel A, Bühler Y, "Intercomparison of photogrammetric platforms for spatially continuous snow depth mapping," The Cryosphere, pp. 69–94, 2021
DOI:https://doi.org/10.5194/tc-15-69-2021

[17] Grisetti G, Grzonka S, Stachniss C, Pfaff P, Burgard W, "Efficient estimation of accurate maximum likelihood maps in 3D," International Conference on Intelligent Robots and Systems, pp.3472–3478, 2017
DOI: https://ieeexplore.ieee.org/document/4399030